Journal of Radioanalytical and Nuclear Chemistry (2021) 330:1485–1495
https://doi.org/10.1007/s10967-021-07954-y

Quantification of ^{222}Rn/ ^{220}Rn exhalation rates from soil samples of Champawat region in Kumaun Himalaya, India

Taufiq Ahamad[1] · Prakhar Singh[2] · O. P. Nautiyal[2] · Manish Joshi[3] · A. A. Bourai[4] · A. S. Rana[1] · Kuldeep Singh[5]

Received: 4 May 2021 / Accepted: 13 August 2021 / Published online: 22 August 2021

Abstract
The present study is carried out in selected locations of the Champawat district in the lesser Kumaun Himalayan belt of Uttarakhand, India. The Scintillation detector-based portable Smart RnDuo monitor was used to estimate exhalation rates of ^{222}Rn and ^{220}Rn. The levels of gamma dose rates were also measured using a portable radiation survey meter at each of the selected locations. The mass exhalation rate for ^{222}Rn varies between 7.8 ± 0.1 and 107.3 ± 2.1 mBq kg^{-1} h^{-1} with an average of 38.9 ± 18.9 mBq kg^{-1} h^{-1}. In contrast, the ^{220}Rn surface exhalation rate ranges from 0.7 ± 0.5 to 14.3 ± 0.7 Bq m^{-2} s^{-1}with an average 6.2 ± 3 Bq m^{-2} s^{-1} and emanation rate was found to range 88.4 and 1703.7 mBq kg^{-1} s^{-1} with an average 739 ± 356.7 mBq kg^{-1} s^{-1}. The gamma dose rate was found to vary from 0.08 ± 0.01 to 0.30 ± 0.03 µSv h^{-1} with an average of 0.18 ± 0.06 µSv h^{-1} in the region.

Keywords Natural background radiation · Smart RnDuo monitor · Exhalation rates · Gamma dose rate

Introduction

Soil, water and air are different phases contributing towards the distribution of natural background radioactivity to the ambient environment of inhabitants with abundantly available radioactive minerals as the significant source term [1–8]. Natural background radiation dose values are reported in a number of studies performed in different parts of the globe [9–12]. Radon (^{222}Rn) and its isotope thoron (^{220}Rn) are the disintegrated products of radium (^{226}Ra) and (^{232}Th), respectively. These gaseous (^{222}Rn and ^{220}Rn) are found throughout the earth's crust in varying concentrations. It has been found that ^{222}Rn, ^{220}Rn and their decay products contribute more than 50% of the total dose to the inhabitants from natural background radiation sources [13].

The amount of radon and thoron in the indoor air is directly related to the presence of the radium (^{226}Ra) and thorium (^{232}Th) radionuclides in soil. Rate of radon exhalation from the soil was observed to be positively linked with indoor radon concentration and radium content in soil [14–16]. Radon and thoron gases are formed by the disintegration of radium and thorium, respectively in the earth's crust. These radioactive gases come to the upper surface of the atmosphere through exhalation and emanation processes. Emanation is a process by which ^{222}Rn atoms escape from the solid mineral grains to the air-filled pores in the soil matrix. In contrast, exhalation is the process by which radon gas is transported from air-filled pores to the earth's atmosphere. The primary contributors to the levels of radon (^{222}Rn)/thoron (^{220}Rn) concentration in the indoor air and outdoor atmosphere are both the source terms, i.e., exhalation and emanation from soil and building materials [17–20].

Radon/thoron is easily transported from the grain particles to the soil pore space (i.e., emanation) and from air-filled pores to the environment or indoor air (exhalation). Diffusion and advection processes can move radon from the pore space to the soil-air interface. However, in the vast majority of cases, radon is transported through diffusion.

✉ Taufiq Ahamad
taufiqahamad1507@gmail.com

[1] Department of Physics, Shri Guru Ram Rai PG College, Dehradun 248001, India

[2] Uttarakhand Science Education and Research Centre, Dehradun 248001, India

[3] Radiological Physics and Advisory Division, Bhabha Atomic Research Center, Mumbai 400094, India

[4] Department of Physics, HNB Garhwal University, BadshahiThaul Campus, Tehri Garhwal 249199, India

[5] Department of Physics, Govt. PG College, Tehri Garhwal, New Tehri 249001, India

The radon is released into the atmosphere after emanation and transportation within the soil [21].

There are several factors which influence radon emanation and exhalation from soil or rock, including radium distribution, grain size, porosity, moisture content, and so on. All of these have a significant impact on the exhalation and emanation process [22–25]. Radium distribution and its relationship to radon exhalation rate and soil-gas radon concentrations are likely to vary in various formations and rock types [26]. Moreover, the external radiation that arises due to exhalation from terrestrial radioactive residues accounts for around 20% of the natural radiation dose [27]. As radon gas is inhaled, densely ionising alpha particles emitted from short-lived radon decay products (^{218}Po and ^{214}Po) interact with biological tissues causing lungs damage [19]. If the concentration of radon, thoron and its daughter products in the closed spaces such as houses, large buildings, and mines exceeds the threshold, it may pose a radiation hazard to the occupants [28–30].

In the present study, radon mass exhalation rate and thoron surface exhalation rate were measured in Champawat region of Kumaun Himalaya, Uttarakhand, India. The ambient gamma dose rates were measured using a portable radiation survey meter at each sampling location. The results of the measurements of exhalation rates in the current work would provide an essential link with indoor radon, thoron and their progeny concentrations in the region. The results of the present study may be helpful in future studies in the field of environmental radioactivity.

Study area

The present study was conducted in the Champawat region which lies in the vicinity of the Kumaun Himalaya, Uttarakhand, India. The Champawat district is located in the southern part of Uttarakhand state (28°N to 29.5° N and 79.7° 34′ E to 80.3° E) and shares an international border with Nepal in the East (Fig. 1). Champawat district covers a total area of 1765.8 Km^2 with an average altitude of

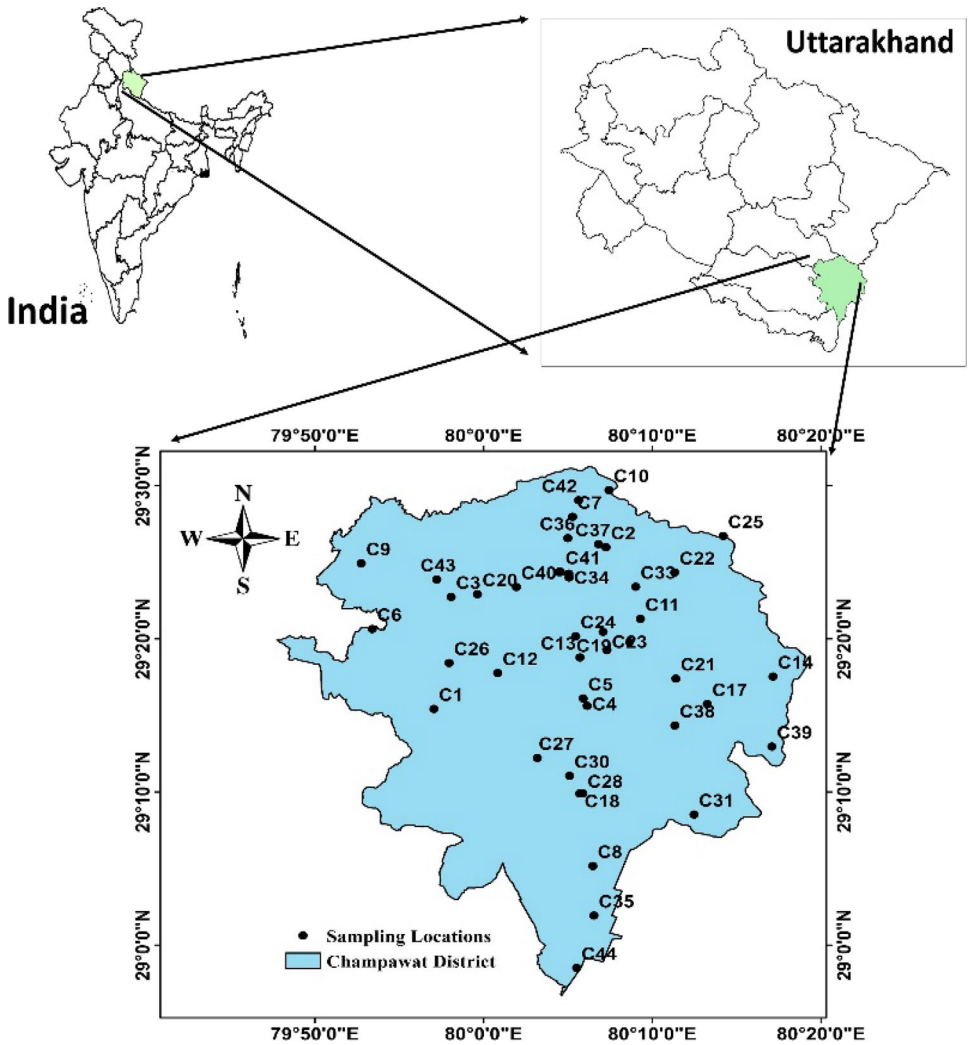

Fig. 1 Map of the study area showing sampling locations

1670 m above sea level. The Kali River divide Uttarakhand and Nepal in the East. The Ladhiya and Lohawati Rivers are the major drainage system in the area. The route from south to north traverses across Bhabhar Formation, Siwalik Group of rocks, Bhimtal Quartzites and Almora Crystallines. Significant tectonic plates such as the Himalayan Frontal Thrust (HFT), Main Boundary Thrust (MBT), and South Almora Thrust (SAT) distinguish the geological formations Current-bedded quartzite with associated volcanic, mica-talc schist, limestone, conglomerate, slate, quartzite, granodiorite, augen gneiss, migmatite, and granite gneiss are found in various parts of the Champawat district. Champawat area is characterized by various units viz. Alluvium plain, Siwalik Group, Outer Lesser Himalaya and the Almora Crystalline unit [31, 32].

Materials and methodology

Measurements of ^{222}Rn/ ^{220}Rn exhalation rates

^{222}Rn and ^{220}Rn exhalation rates from soil were measured using a scintillation detector based Smart RnDuo radon monitor. The Smart RnDuo is a real-time portable radon monitor. The alpha scintillations from radon and its decay products are counted via a photo multiplier tube (PMT) and the associated counting electronics. The Smart RnDuo has a quick reaction time and operates in a permanent, maintenance-free mode with long-term calibration stability and suitable for radon monitoring in both indoor as well as outdoor conditions. This equipment can be used to test radon levels in soil, water, and the Naturally Occurring Radioactive Materials (NORMs). The detection limit of Smart RnDuo ranges from 8 Bq m^{-3} to 50 MBq m^{-3} [33]. The investigations for the present study were carried out in the different areas situated in the entire Champawat district of Kumaun Himalaya, India. The detailed description of measurement procedures of surface and mass exhalation rates is given below. The gamma dose rates were also measured using a radiation survey meter manufactured by ATOMTEX (Belarus) at each sampling location.

Measurements of thoron surface exhalation rates

The Smart RnDuo monitor was employed to measure thoron surface exhalation rates. Thoron is not uniformly distributed in the accumulation chamber on account of its very short diffusion length. Therefore, the Smart RnDuo monitor was operated in flow mode to estimate surface exhalation of thoron. Smart RnDuo has an in-built function for the flow mode operation. It sets the pump ON automatically for 5 min in 15 min cycle or 15 min in 1-h cycle, respectively. To measure ^{220}Rn surface exhalation rates, 15 min cycles were taken and the air volume in the chamber was kept to a minimum to ensure proper air mixing inside the closed-loop. The measurement procedure of thoron surface exhalation is shown in Fig. 2. The detailed measurement principle can found in the literature [34, 35]. For calculating the steady-state ^{220}Rn concentration (Bq m^{-3}), the averages of four values were considered for the estimation. The Eq. (1) is used to calculate the surface exhalation rate (J_S)

$$J_S = C_T V \lambda / A \tag{1}$$

where, C_T represents the average concentration of thoron inside the accumulation chamber (Bq m^{-3}), V, λ and A are the residual air volume (m^3), effective decay constant for ^{220}Rn (h^{-1}) and the surface area of the chamber (m^2), respectively. The mass emanation rate of ^{220}Rn from soil can be determined using Eq. (2) [36]

$$J = [J_S/(\rho \times L_S)]\tanh\left(Z_S/L_S\right) \tag{2}$$

where, J_S = surface exhalation rate, Z_S = sample height, Ls = diffusion length of ^{220}Rn within soil and ρ = density of soil samples. The ratio Z_s/L_s is greater than unity since the diffusion of thoron (L_s) is about 1 cm [37]. Using this approximation, Eq. (2) can be represented as

$$J = J_S/(\rho \times L_S) \tag{3}$$

The Eq. (3) is used to estimate thoron mass exhalation rate.

Measurement of mass exhalation rate of ^{222}Rn

The soil samples (each sample ≈ 1 kg) were collected from the ground at a depth of 30 cm and dried under the sunlight. The roots, stones, peebles were removed from the ground surface before collecting the samples. The measurements of radon mass exhalation rates in the collected samples were carried out in the laboratory.

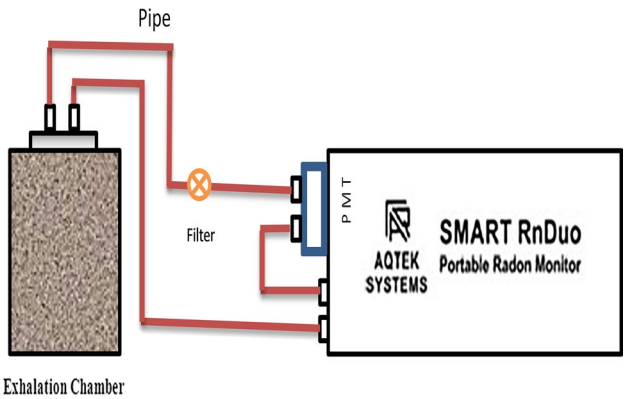

Fig. 2 Schematic diagram in Flow mode of Smart RnDuo for surface exhalation measurement

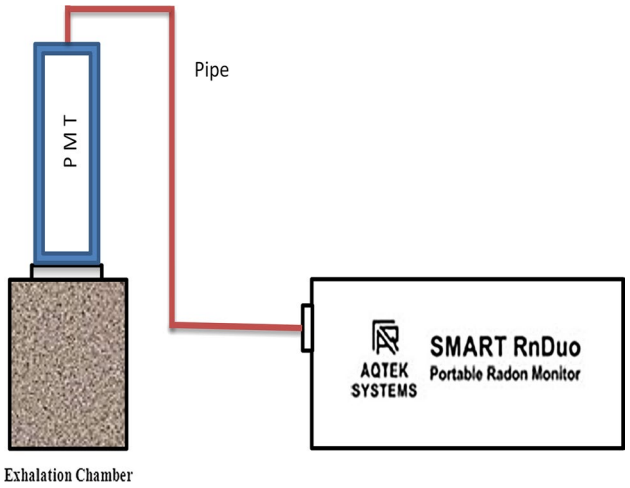

Fig. 3 Schematic diagram in diffusion mode for Mass Exhalation Using Smart RnDuo

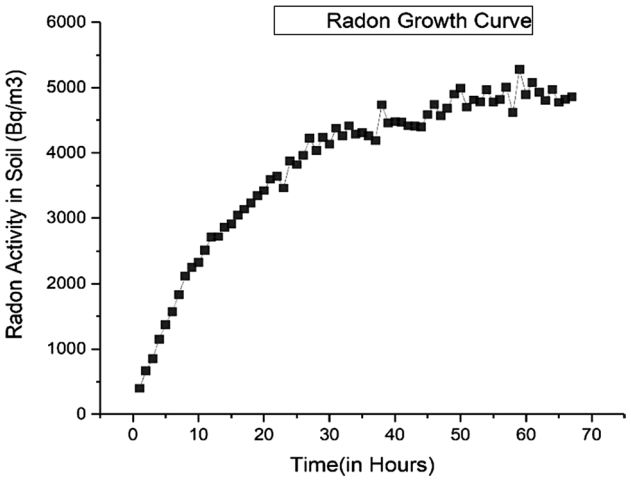

Fig. 4 Growth curve of Accumulated Radon

The schematic diagram of the measurement procedure is shown in Fig. 3. The Smart RnDuo monitor is connected to a close cylindrical and leakage-free accumulation chamber made of stainless steel. For ^{222}Rn measurement, the Smart RnDuo monitor was programmed to run for 24 h on a 60-min cycle. The monitor is operated in diffusion mode to avoid the thoron interferences since thoron has a very short diffusion length as compared to that of radon. The detailed explanation of the Smart RnDuo as well as the measuring technique is given elsewhere [33]. The growth of radon concentration C_t at time t (Bq m^{-3}) in the accumulated chamber is given by following Eq. (4)

$$C_t = \left(J_m M/V\lambda_e\right)\left[1-e^{-\lambda et}\right] + C_0 e^{-\lambda et} \quad (4)$$

where, C_t, J_m, M, V, and λ_e represent the concentration of ^{222}Rn at any time t (Bq m^{-3}), mass exhalation rate (Bq kg^{-1} h^{-1}), sample mass (kg), volume of the chamber plus scintillation cell (m^3), effective decay constant (h^{-1}) which is the summation of leakage rates of ^{222}Rn and decay constant of the accumulator if it exits. At $t=0$, C_0 represents initial ^{222}Rn concentration in the chamber. The data is further linearly fitted as per the Eq. (4) to obtain mass exhalation rate (J_m).

In linear approximation, Eq. (4) can be transformed into the following Eq. (5)

$$C_t = \left(J_m M/V\right)t + C_0 \quad (5)$$

The graph was plotted between radon concentration data (Bq m^{-3}) with time (in hour) and it gives the well-known exponential growth curve of radon accumulation as shown in Fig. 4 [38, 39].

Measurements of gamma dose rate

The Radiation Survey Meter manufactured by ATOMTEX (Belarus) was used to measure the gamma dose rates. Gamma dose rate were measured 1 m above the ground surface at all sampling locations. The gamma dose rate survey may be hepful in the estimation of terrestrial radiation in the study area.

Result and discussion

^{222}Rn mass exhalation rate from the soil samples

Table 1 represents the measured values of gamma dose rate (μSv h^{-1}), ^{222}Rn mass exhalation rate (mBq kg^{-1} h^{-1}), ^{220}Rn Surface exhalation rate (Bq m^{-2} s^{-1}) and ^{220}Rn emanation rate (mBq kg^{-1} s^{-1}) for collected samples and statistical parameters (minima, maxima, mean and standard deviation.

The values of ^{222}Rn mass exhalation rate varied from 7.8 ± 0.1 to 107.3 ± 2.1 mBq kg^{-1} h^{-1}with an average of 38.9 ± 18.9 mBq kg^{-1} h^{-1}. Topological studies show that the high exhalation rate from the soil matrix causes a high level of terrestrial radiation exposure [40]. The higher value of ^{222}Rn mass exhalation rate can be attributed to the higher ^{226}Ra content in the soil samples. The high values of mass exhalation rates were found for samples C10, C13, C41, C42, C43 and C44. These specific high values are caused by high radium content in the porous soil matrix. The low values of mass exhalation rates correspond to samples C2 and C4. The different geological formations and soil composition tend to obtain different exhalation rates determined by the abundance of parent source term [41]. The formation alongside the main boundary thrust (MBT) like sand-stone bedrock and mudstone is also

Table 1 The observed values of Gamma dose rates and Exhalation rates of ^{222}Rn and ^{220}Rn in the soil from Champawat region, Uttarakhand

Sample no.	Gamma dose rate (μSv h^{-1})	Mass exhalation rate J_m (mBq kg^{-1} h^{-1})	Surface exhalation rate J_s (Bq m^{-2} s^{-1})	Emanation rate (mBq kg^{-1} s^{-1})
C1	0.26 ± 0.03	35.3 ± 0.9	9.6 ± 0.5	1149.5
C2	0.15 ± 0.01	7.8 ± 0.1	10.7 ± 0.5	1251.4
C3	0.18 ± 0.02	26.6 ± 0.5	7.4 ± 0.4	883.0
C4	0.18 ± 0.01	15.2 ± 0.4	2.7 ± 0.3	333.2
C5	0.17 ± 0.01	36.0 ± 0.3	5.1 ± 0.4	611.5
C6	0.18 ± 0.01	40.1 ± 0.3	1.4 ± 0.2	161.0
C7	0.15 ± 0.01	31.4 ± 0.7	6.3 ± 0.1	756.3
C8	0.20 ± 0.02	41.2 ± 0.2	2.5 ± 0.3	297.1
C9	0.19 ± 0.02	41.4 ± 0.3	8.8 ± 0.5	1047.5
C10	0.21 ± 0.02	82.1 ± 0.8	14.3 ± 0.7	1703.7
C11	0.27 ± 0.02	24.5 ± 0.5	7.9 ± 0.6	940.5
C12	0.30 ± 0.04	46.5 ± 1.5	7.3 ± 0.6	870.3
C13	0.18 ± 0.02	76.1 ± 0.2	5.1 ± 0.5	611.5
C14	0.09 ± 0.02	28.5 ± 0.5	1.5 ± 0.6	178.9
C15	0.08 ± 0.02	38.5 ± 0.3	7.1 ± 0.4	845.6
C16	0.08 ± 0.02	20.2 ± 0.1	2.7 ± 0.6	324.6
C17	0.10 ± 0.03	20.8 ± 0.4	9.2 ± 0.7	1094.6
C18	0.15 ± 0.02	44.9 ± 0.1	12.1 ± 0.7	1451.0
C19	0.13 ± 0.01	28.5 ± 0.2	7.3 ± 0.6	875.3
C20	0.22 ± 0.01	25.6 ± 0.1	8.5 ± 0.6	1020.0
C21	0.15 ± 0.01	28.2 ± 0.3	7.5 ± 0.3	898.4
C22	0.15 ± 0.01	19.4 ± 0.3	8.6 ± 0.5	1025.2
C23	0.19 ± 0.02	28.2 ± 0.6	5.1 ± 0.6	608.6
C24	0.18 ± 0.02	34.5 ± 0.5	1.1 ± 0.6	131.4
C25	0.22 ± 0.01	44.6 ± 0.1	6.5 ± 0.6	774.0
C26	0.10 ± 0.01	21.1 ± 0.2	0.7 ± 0.5	88.4
C27	0.08 ± 0.01	32.5 ± 0.1	3.8 ± 0.4	449.6
C28	0.21 ± 0.01	47.5 ± 1.3	9.5 ± 0.5	1132.7
C29	0.22 ± 0.03	27.3 ± 0.6	5.6 ± 0.7	671.5
C30	0.18 ± 0.02	40.9 ± 0.5	4.3 ± 0.3	513.8
C31	0.24 ± 0.03	46.5 ± 0.6	4.4 ± 0.2	531.0
C32	0.21 ± 0.02	35.7 ± 0.1	6.4 ± 0.1	767.7
C33	0.22 ± 0.02	34.8 ± 0.7	6.5 ± 0.6	778.5
C34	0.19 ± 0.02	41.9 ± 1.0	7.5 ± 0.4	907.7
C35	0.23 ± 0.02	36.7 ± 0.7	10.5 ± 0.3	1251.9
C36	0.16 ± 0.01	28.2 ± 0.8	6.7 ± 0.4	804.3
C37	0.14 ± 0.01	29.8 ± 0.4	3.3 ± 0.4	393.1
C38	0.14 ± 0.01	35.2 ± 0.4	2.5 ± 0.4	297.1
C39	0.17 ± 0.02	35.6 ± 0.5	3.9 ± 0.5	467.6
C40	0.21 ± 0.02	46.0 ± 1.2	5.4 ± 0.4	640.3
C41	0.24 ± 0.01	62.9 ± 1.4	6.0 ± 0.5	719.3
C42	0.30 ± 0.03	107.3 ± 2.1	4.1 ± 0.3	495.0
C43	0.27 ± 0.02	87.0 ± 2.1	6.0 ± 0.3	712.0
C44	0.15 ± 0.01	49.4 ± 1.1	8.8 ± 0.4	1048.2
Min	0.08 ± 0.01	7.8 ± 0.1	0.7 ± 0.5	88.4
Max	0.30 ± 0.03	107.3 ± 2.1	14.3 ± 0.7	1703.7
Avg	0.18	38.9	6.2	739.0
SD	0.06	18.9	3.0	356.7

responsible for such vast variation for a small region [42]. The Fig. 5 shows the statistical distribution of ^{222}Rn mass exhalation rates of the samples.

The Box plot on the left shows that the mean is about 39 mBq kg^{-1} h^{-1} and the median is about 35 mBq kg^{-1} h^{-1}. The measured ^{222}Rn mass exhalation rate of 25% and 75% of the samples is below and above 30 mBq kg^{-1} h^{-1}, respectively (Fig. 5). The mean occurs in the third quartile that shows a higher mean value than the median value. The right side of the plot shows the kernel density of the data and the statistical distribution is approximated to a normal distribution. However, the dataset has a negative skewness because large numbers of the data points are lying beyond the central area of the kernel density. This indicates a wide distribution of ^{222}Rn mass exhalation rate over the area.

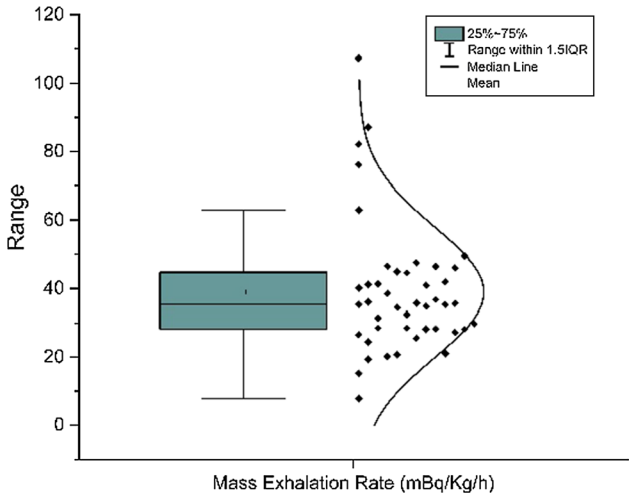

Fig. 5 Box plot representing the statistics of mass exhalation data

^{220}Rn surface exhalation rate and emanation rate

The measured values of ^{220}Rn surface exhalation rate (Bq m^{-2} s^{-1}) and emanation rate (mBq kg^{-1} s^{-1}) along with their statistical parameters (minima, maxima, mean and standard deviation), are shown in Table 1. The measured levels of surface exhalation of ^{220}Rn vary from 0.7 ± 0.5 and 14.3 ± 0.7 Bq m^{-2} s^{-1} with an average of 6.2 ± 3 Bq m^{-2} s^{-1} the different locations of Champawat. The higher levels of ^{220}Rn surface exhalation rate might be attributed to the higher concentration of thorium content in the soil profiles. The results due to higher levels of ^{220}Rn surface exhalation are comparable with the other studies in the Northern part of India as shown in Table 2. There were 44 soil samples collected from different locations in the investigated region, among them 52% samples indicate higher surface exhalation rate than the average value 6.2 ± 3 Bq m^{-2} s^{-1}. The thoron emanation rate was to be found between 88.4 and 1703.7 mBq kg^{-1} s^{-1} with an average 739 ± 356.7 mBq kg^{-1} s^{-1}. Different diffusion lengths of thoron cause variation in mass emanation rate. The diffusion length depends upon the porosity of the soil matrix. Figure 6 shows the Whisker's plot of ^{220}Rn surface exhalation rate which indicates the statistical summary of the data. The median is slightly higher than the mean but can be approximated equally. This is the characteristic of a normal distribution with a fine goodness-of-fit but with some skewness. The right side of the plot shows a good approximation of the normal distribution for the dataset. Thoron surface exhalation rate of 25% of the samples was observed below 4 Bq m^{-2} s^{-1}. Figure 7 shows a Whisker's diagram of ^{220}Rn emanation rate dataset. The mean of the dataset occurs in the second quartile of the Whisker's box, indicating that the median is higher than the mean. The emanation rate of 25% of the samples was found below 500 mBq kg^{-1} s^{-1}. The right side of the plot shows the kernel density of the dataset which shows that the whole data follows normal distribution like mass exhalation rate and surface exhalation rate.

Table 2 Comparision of radon mass exhalation rates and thoron surface exhalation rates with previous studies from Northern India

Study region	Radon mass exhalation rate (mBq kg^{-1} h^{-1})		Thoron surface exhalation rate (Bq m^{-2} s^{-1})		References
	Max	Min	Max	Min	
Jammu region	38	15	1.35	0.02	[43]
Haryana	63.5	58.6	0.03×10^{-3}	–	[44]
Punjab	0.0382	0.0169	–	–	[46]
Himachal Pradesh	91.2	28.2	0.05×10^{-3}	0.01×10^{-3}	[45]
Almora (Uttarakhand)	54	16	6.4	0.7	[41]
Bageshwar (Uttarakhand)	67	11.9	7.3	0.2	[40]
Dehradun & Haridwar (Uttarakhand)	110.8	15.9	3.1	0.8	[47]
Champawat (Uttarakhand)	107.3	7.80	14.3	0.7	Present Study

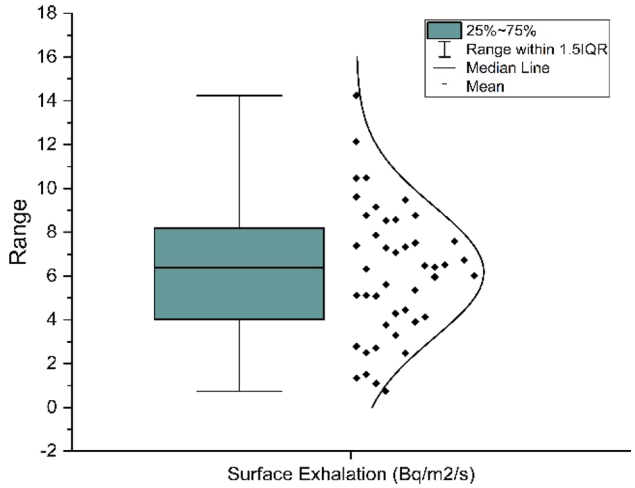

Fig. 6 Box plot representing the statistics of surface exhalation data

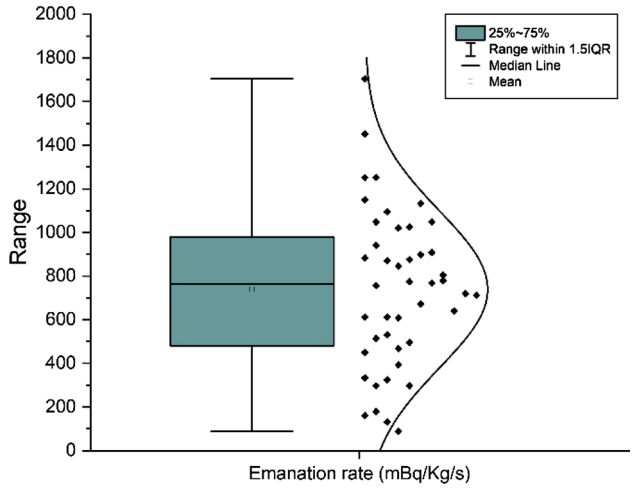

Fig. 7 Box plot representing the statistics of mass emanation data

Gamma dose rates

The Gamma dose rates were measured at the same locations of study area from where the soil samples were collected and the measured values are shown in Table 1. The Gamma dose rate varies from 0.08 ± 0.01 to 0.30 ± 0.03 μSv h^{-1} with an average 0.18 ± 0.06 μSv h^{-1}. Gamma dose rate gives a background radiation level due to all types of radiation sources, i.e., terrestrial and cosmic radiation.

Spatial distribution of ^{222}Rn exhalation rate and ^{220}Rn exhalation rate

Figure 8 shows the spatial distribution of ^{222}Rn mass and ^{220}Rn surface exhalation rate of the soil samples taken from the study area i.e., Champawat district of Uttarakhand State of India. As the dataset is pointwise located on the map of Champawat, the neighboring values were determined using inverse distance weightage approximation. The spatial distribution is then denoted with the colour-coded contouring intervals. This method does not provide the actual values on neighboring locations but gives a general idea of the approximate values on the locations from where the samples were not taken. In Fig. 8a the soil samples taken from locations C10, C42 and C43 show the higher values of ^{222}Rn mass exhalation rate and the region in between shows the lower values (below 20 mBq kg^{-1} h^{-1}). Figure 8b shows that most of the region occurs at high surface exhalation rates and locations C2, C10, C18 and C35 have the highest values of J_s (i.e., 10.5–14.3 Bq m^{-2} s^{-1}). This indicates the possibility of a high abundance of thorium over the region.

Correlation study

The Fig. 9 shows a correlation matrix indicating the mutual correlations of gamma dose rate, ^{222}Rn mass exhalation rate, ^{220}Rn surface exhalation rate and ^{220}Rn emanation rate. The radon mass exhalation rate in the soil is plotted against thoron surface exhalation rates. A weak positive correlation with Pearson's value 0.10 was observed between radon mass exhalation rate and thoron surface exhalation rate. A significant correlation was found between the gamma dose rate and the radon mass exhalation rate with Pearson's value of 0.51. No significant correlation was observed between gamma dose rate and thoron surface exhalation rate with Pearson's value of 0.22. A strong positive correlation was found between emanation rate and surface exhalation rate of thoron with Pearson's value of 1. It indicates an obvious and significant relationship between the surface exhalation rate and emanation rate of thoron [40, 41]. Emanation rates are showing the same trends of correlation with other entities, same as surface exhalation rate. The diagonal graphs show the histograms over the datasets, which provides the statistical distribution of the datasets.

Comparison with previous studies

Table 2 represents values of radon mass exhalation rates and thoron surface exhalation rates previously reported in different parts of northern India. Similarly, Table 3 shows the values of radon mass exhalation rates and thoron surface exhalation rates in different regions of the globe. The average value of ^{222}Rn mass exhalation rate estimated in the investigated region is comparable with the recent studies, as shown in Tables 2 and 3. The ^{220}Rn surface exhalation rate is found to be significantly higher than the values reported in other studies.

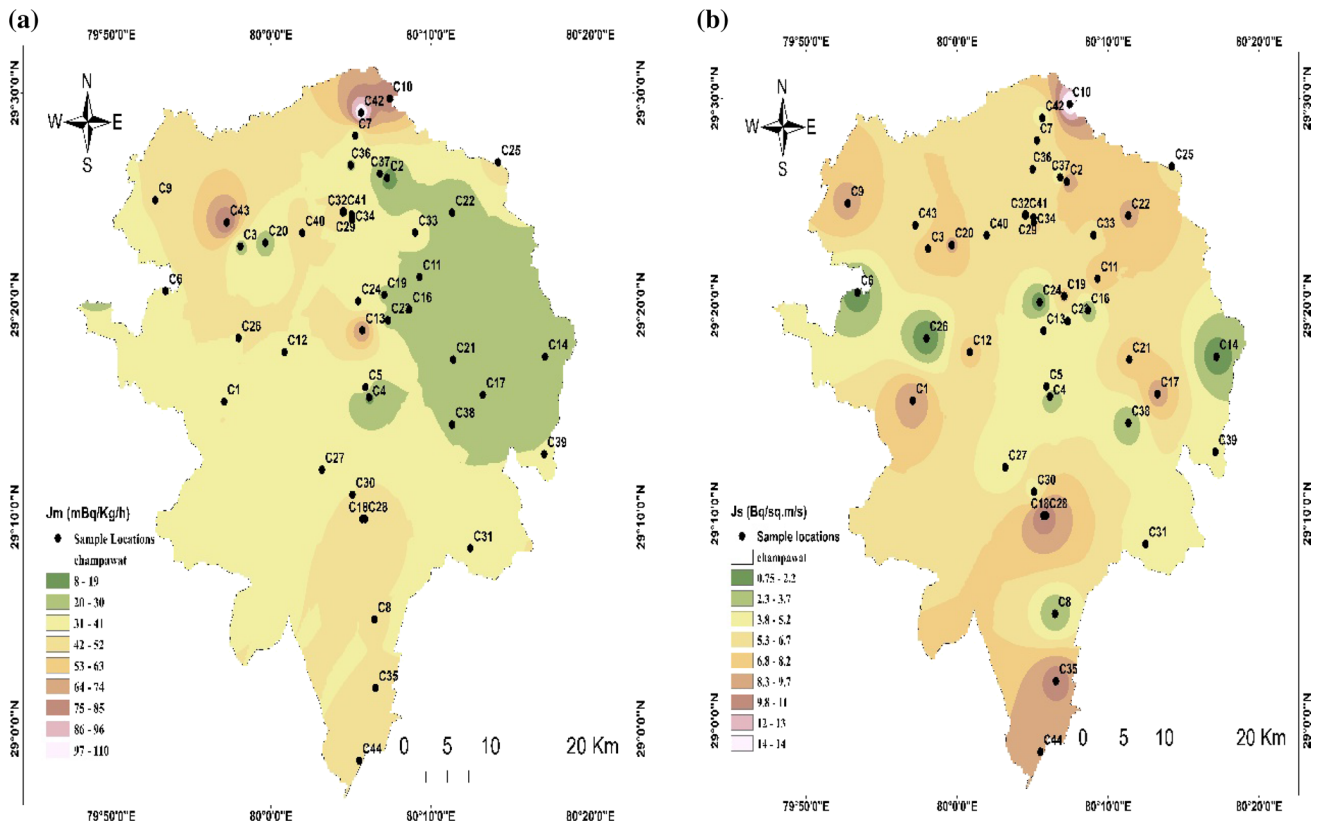

Fig. 8 Spatial distribution of **a** ^{222}Rn exhalation rate and **b** ^{220}Rn exhalation rate

Conclusions

The study shows that the exhalation rates of ^{222}Rn and ^{220}Rn in the soil are controlled by several factors like porosity, geological features, and minerals present in the soil. However, Main Boundary Thrust (MBT) and local faults might have played a significant role in controlling exhalation and emanation rates in the study area. The average gamma dose rate was found 0.18 ± 0.06 μSv h^{-1}. The average mass exhalation rate in the study area was found to be 38.9 ± 18.9 mBq kg^{-1} h^{-1} which is less than the global average 57 mBq kg^{-1} h^{-1}. The observed variation may depend on the uranium mineralization in the study area. The high surface exhalation rate indicating rich thorium content in the study area has an average of 6.2 ± 3 Bq m^{-2} s^{-1}. A weak positive correlation observed between mass exhalation rate and surface exhalation rate can be linked to shorter half-life and diffusion lenght for thoron. Most of the samples have shown higher surface exhalation rate than the global average value 1 Bq m^{-2} s^{-1}, which is in close agreement with more elevated surface exhalation rate in northern part of India (Table 2). A strong correlation coefficient between the thoron emanation and thoron surface exhalation rate shows that the exhalation rate depends on emanation. The results of the present study will be helpful to substantiate the measurements of radon, thoron and progeny levels in the study area.

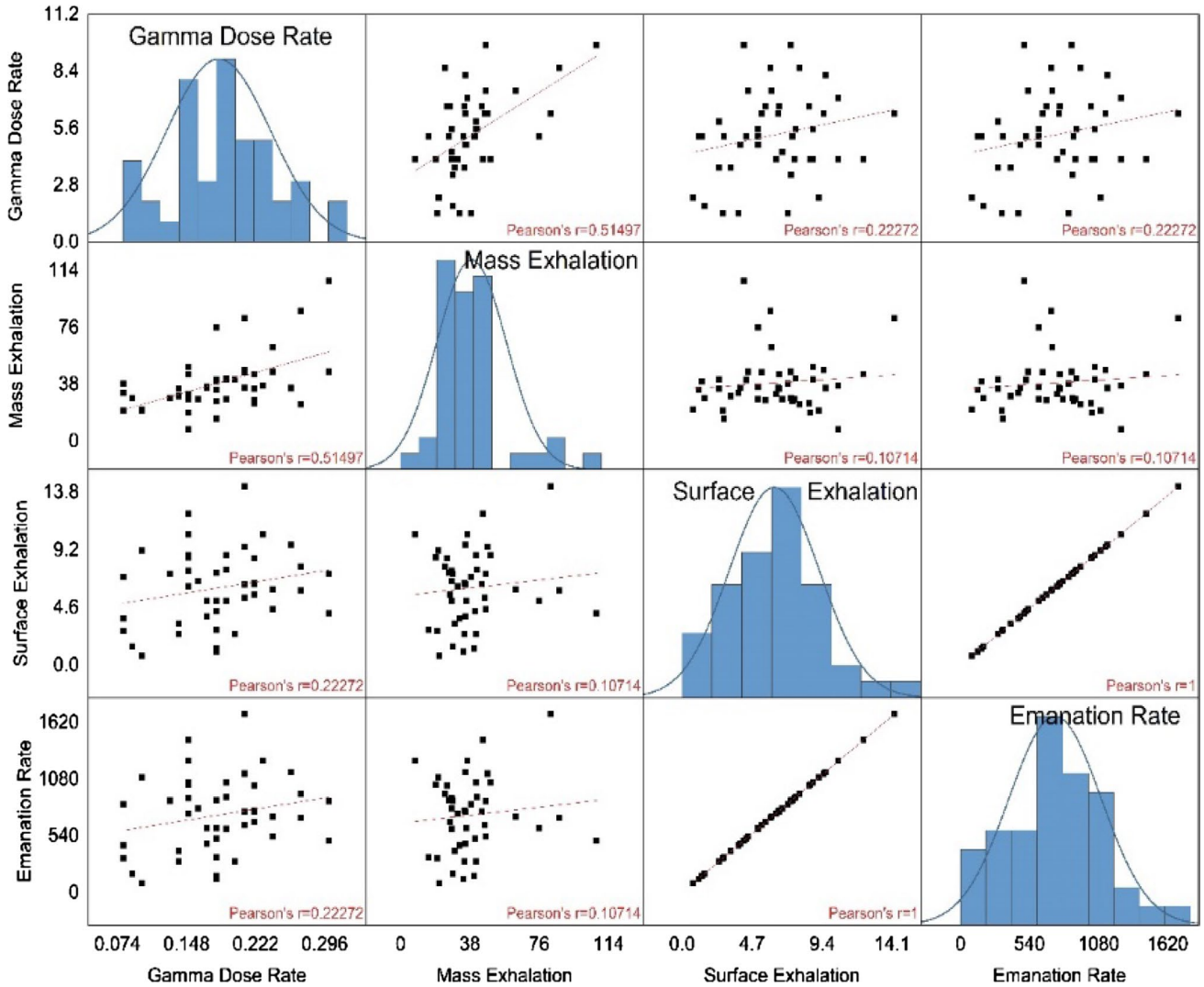

Fig. 9 Matrix plot representing Pearson correlations of the statistical data

Table 3 Comparision of radon mass exhalation rates and thoron surface exhalation rates with some worldwide studies

Study region	Radon mass exhalation rate (mBq kg^{-1} h^{-1})		Thoron surface exhalation rate (Bq m^{-2} s^{-1})		References
	Max.	Min.	Max.	Min.	
Southern Turkey	253.2	35.76	1.43×10^{-3}	0.63×10^{-3}	[48]
Serbia	11.4	1.3	0.23×10^{-3}	0.38×10^{-3}	[49]
Egypt	600	50	4.32×10^{-3}	0.35×10^{-3}	[50]
Sudan	11.25	2.84	0.26×10^{-3}	0.06×10^{-3}	[51]
Baghdad, Iraq	210	90	2.75×10^{-3}	0.12×10^{-3}	[52]
Champawat (Uttarakhand)	107.3	7.8	14.3	0.7	Present Study

Acknowledgements The authors acknowledge the Board of Research in Nuclear Science (BRNS), Department of Atomic Energy (DAE) Project Ref. 36(4)/14/46/2016-BRNS, Mumbai, India, for extending their laboratory facilities for conducting the experimental work and financial support for the research work.

Declarations

Conflict of interest The authors declare that they have no conflict of interest in this manuscript.

References

1. Nazaroff WW, Nero AV (1988) Radon and its decay products in indoor air. Wiley, New York
2. Ramola RC, Prasad M, Kandari T, Pant P, Bossew P, Mishra R, Tokonami S (2016) Dose estimation derived from the exposure to radon, thoron and their progeny in the indoor environment. Sci Rep 6(1):1–16
3. Bangotra P, Mehra R, Kaur K, Jakhu R (2016) Study of natural radioactivity (226Ra, 232Th and 40K) in soil samples for the assessment of average efective dose and radiation hazards. Radiat Prot Dosim 171(2):277–281. https://doi.org/10.1093/rpd/ncw074
4. Kandari T, Prasad M, Pant P, Semwal P, Bourai AA, Ramola RC (2018) Study of radon fux and natural radionuclides (226Ra, 232Th and 40K) in the main boundary thrust region of Garhwal Himalaya. Acta Geophys 66:1243–1248
5. Prasad Y, Prasad G, Gusain GS, Choubey VM, Ramola RC (2009) Seasonal variation on radon emission from soil and water. Indian J Phys 83(7):1001–1010
6. Akpanowo M, Umaru I, Iyakwari S, Joshua EO, Yusuf S, Ekong GB (2020) Determination of natural radioactivity levels and radiological hazards in environmental samples from artisanal mining sites of Anka. North-West Nigeria Sci African 10:e00561. https://doi.org/10.1016/j.sciaf.2020.e00561
7. Shahrokhi A, Adelikhah M, Chalupnik S, Kovács T (2021) Multivariate statistical approach on distribution of natural and anthropogenic radionuclides and associated radiation indices along the north-western coastline of Aegean Sea, Greece. Mar Pollut Bull 163:112009. https://doi.org/10.1016/j.marpolbul.2021.112009
8. Thu HNP, Thang NV, Loan TTH, Dong NV, Hao LC (2019) Natural radioactivity and radon emanation coefficient in the soil of Ninh Son region, Vietnam. Appl Geochem 104:176–183. https://doi.org/10.1016/j.apgeochem.2019.03.019
9. Bezuidenhout J (2021) Estimating indoor radon concentrations based on the uranium content of geological units in South Africa. J Environ Radioact 234:106647. https://doi.org/10.1016/j.jenvrad.2021.106647
10. Shahrokhi A, Adelikhah M, Imani M, Kovács T (2021) A brief radiological survey and associated occupational exposure to radiation in an open pit slate mine in Kashan, Iran. J Radioanal Nucl Chem. https://doi.org/10.1007/s10967-021-07778
11. Mehra R, Jakhu R, Bangotra P, Kaur K, Mittal HM (2016) Assessment of inhalation dose from the indoor 222Rn and 220Rn using RAD7 and pinhole cup dosemeters. Radiat Prot Dosim 171(2):208–211
12. Prasad M, Bossew P, Kumar GA, Mishra R, Ramola RC (2018) Dose assessment from the exposure to attached and unattached progeny of radon and thoron in indoor environment. Acta Geophys 66(5):1187–1194
13. UNSCEAR (2000) Sources and effects of ionizing radiation. United Nation Scientific Committee on the Effects of Atomic Radiation, New York
14. Kumar A, Singh P, Semwal P, Singh K, Prasad M, Ramola RC (2021) Study of primordial radionuclides and radon/thoron exhalation rates in Bageshwar region of Kumaun Himalaya, India. J Radioanal Nucl Chem 328(3):1361–1367
15. Gusain GS, Prasad G, Prasad Y, Ramola RC (2009) Comparison of indoor radon level with radon exhalation rate from soil in Garhwal Himalaya. Radiat Meas 44(9–10):1032–1035
16. Ramola RC, Choubey VM (2003) Measurement of radon exhalation rate from soil samples of Garhwal Himalaya, India. J Radioanal Nucl Chem 256(2):219–223
17. Kaur M, Kumar A, Mehra R, Mishra R (2018) Study of radon/thoron exhalation rate, soil-gas radon concentration, and assessment of indoor radon/thoron concentration in Siwalik Himalayas of Jammu & Kashmir. Hum Ecol Risk Assess 24(8):2275–2287
18. Adelikhah M, Shahrokhi A, Imani M, Chalupnik S, Kovács T (2021) Radiological assessment of indoor radon and thoron concentrations and indoor radon map of dwellings in Mashhad, Iran. Int J Environ Res Public Health 18(1):141. https://doi.org/10.3390/ijerph18010141
19. World Health Organization WHO (2009) Handbook on Indoor Radon and A public health perspective
20. Sabbarese C, Ambrosino F, D'Onofrio A (2021) Development of radon transport model in different types of dwellings to assess indoor activity concentration. J Environ Radioact 227:106501
21. Ishimori Y, Lange K, Martin P, Mayya YS, Phaneuf M (2013) Measurement and calculation of radon releases from NORM residues. IAEA
22. Kovács T, Shahrokhi A, Sas Z, Vigh T, Somlai J (2017) Radon exhalation study of manganese clay residue and usability in brick production. J Environ Radioact 168:15–20
23. Shweikani R, Giaddui TG, Durrani SA (1995) The effect of soil parameters on the radon concentration values in the environment. Radiat Meas 25(1–4):581–584
24. Shahrokhi A, Kovacs T (2021) Radiological survey on radon entry path in an underground mine and implementation of an optimized mitigation system. Environ Sci Eur 33(1):1–14
25. Jonas J, Sas Z, Vaupotic J, Kocsis E, Somlai J, Kovacs T (2016) Thoron emanation and exhalation of Slovenian soils determined by a PIC detector-equipped radon monitor. Nukleonika 61(3):379–384
26. Prasad Y, Prasad G, Gusain GS, Choubey VM, Ramola RC (2008) Radon exhalation rate from soil samples of South Kumaun Lesser Himalayas, India. Radiat Meas 43:S369–S374
27. Raghavendra T, Ramakrishna SUB, Vijayalakshmi T, Himabindu V, Arunachalam J (2014) Assessment of radon concentration and external gamma radiation level in the environs of the proposed uranium mine at Peddagattu and Seripally regions, Andhra Pradesh, India. J Radiat Res Appl Sci 7(3):269–273
28. UNSCEAR (2006) United Nations scientific committee on the effects of atomic radiation. Report A/AC.82/-644, exposures of workers and the public from various sources of radiation, United Nations, New York
29. Çelik N, Çevik U, Çelik A, Kucukomeroglu B (2008) Determination of indoor radon and soil radioactivity levels in Giresun, Turkey. J Environ Radioact 99(8):1349–1354. https://doi.org/10.1016/j.jenvrad.2008.04.010
30. Sas Z, Somlai J, Szeiler G, Kovács T (2012) Radon emanation and exhalation characteristic of heat-treated clay samples. Radiat Prot Dosim 152(1–3):51–54
31. Valdiya KS (1980) Geology of the Kumaun Lesser Himalaya. Wadia Institute of Himalayan Geology, Dehradun, India, p 291
32. Kothyari GC, Pant PD, Luirei K (2012) Landslides and neotectonic activities in the main boundary thrust (MBT) zone: Southeastern Kumaun, Uttarakhand. J Geol Soc India 80:101–110
33. Operational manual of Portable radon monitor Smart RnDuo (2015)
34. Gaware JJ, Sahoo BK, Sapra BK (2011) Development of online radon and thoron monitoring systems for occupation and general environments. BARC News Lett 318:45–51

35. Sahoo BK, Mayya YS (2010) Two dimensional diffusion theory of trace gas emission in to soil chambers for flux measurements. Agric For Meteorol 150(9):1211–1224
36. Ujić P, Čeliković I, Kandić A, Žunić Z (2008) Standardization and difficulties of the thoron exhalation rate measurements using an accumulation chamber. Radiat Meas 43:1396–1401. https://doi.org/10.1016/j.radmeas.2008.03.003
37. Mayya YS (2004) Theory of radon exhalation into accumulators placed at the soil–atmosphere interface. Radiat Prot Dosim 111(3):305–318
38. Aldenkamp FJ, De Meijer RJ, Put LW, Stoop P (1992) An assessment of in situ radon exhalation measurements, and the relation between free and bound exhalation rates. Radiat Prot Dosim 45:449–453
39. Sahoo BK, Nathwani D, Eappen KP et al (2007) Estimation of radon emanation factor in Indian building materials. Radiat Meas 42:1422–1425. https://doi.org/10.1016/j.radmeas.2007.04.002
40. Kumar A, Singh P, Agarwal T, Joshi M, Semwal P, Singh K, Pathak PP, Ramola RC (2020) Statistical inferences from measured data on concentrations of naturally occurring radon, thoron, and decay products in Kumaun Himalayan belt. Environ Sci Poll Res 27(32):40229
41. Semwal P, Singh K, Agarwal TK, Joshi M, Pant P, Kandari T, Ramola RC (2018) Measurement of 222 Rn and 220 Rn exhalation rate from soil samples of Kumaun Hills, India. Acta Geophys 66(5):1203–1211
42. Kandari T, Aswal S, Prasad M, Bourai AA, Ramola RC (2016) Estimation of annual effective dose from radon concentration along Main Boundary Thrust (MBT) in Garhwal Himalaya. J Radiat Res Appl Sci 9(3):228–233
43. Kaur M, Kumar A, Mehra R, Mishra R, Bajwa BS (2021) Measurement of radionuclide contents and 222 Rn/220 Rn exhalation rate in soil samples from sub-mountainous region of India. Arab J Geosci 14(9):1–16
44. Kumar A, Chauhan RP, Joshi M, Aggarwal P (2015) Implications of variability in Indoor radon/thoron levels: a study of dwellings in Haryana, India. Environ Earth Sci 73(8):4033–4042
45. Chauhan RP, Kumar A, Chauhan N, Joshi M, Aggarwal P, Sahoo BK (2015) Indoor and built ventilation effect on indoor radon—thoron levels in dwellings and correlation with soil exhalation rates. Indoor Built Environ. https://doi.org/10.1177/1420326X14542887
46. Bangotra P, Mehra R, Jakhu R, Kaur K, Pandit P, Kanse S (2018) Estimation of 222Rn exhalation rate and assessment of radiological risk from activity concentration of 226Ra, 232Th and 40K. J Geochem Explor 184:304–310. https://doi.org/10.1016/j.gexplo.2017.05.002
47. Anamika K, Mehra R, Malik P (2020) Assessment of radiological impacts of natural radionuclides and radon exhalation rate measured in the soil samples of Himalayan foothills of Uttarakhand, India. J Radioanal Nucl Chem 323(1):263–274. https://doi.org/10.1007/s10967-019-06876-0
48. Tabar E, Yakut H, Kuş A (2018) Measurement of the radon exhalation rate and effective radium concentration in soil samples of southern Sakarya, Turkey. Indoor Built Environ 27(2):278–288
49. Stajic JM, Nikezic D (2015) Measurement of radon exhalation rates from some building materials used in Serbian construction. J Radioanal Nucl Chem 303(3):1943–1947
50. Abbas YM, Hegazy TM, Nassif MS, Shoeib MY, Abd-Elraheem AF (2020) Measurement of 226Ra concentration and radon exhalation rate in rock samples from Al-Qusair area using CR-39. J Radiat Res Appl Sci 13(1):102–110. https://doi.org/10.1080/16878507.2019.1706264
51. Elzain AEA (2015) Radon exhalation rates from some building materials used in Sudan. Indoor Built Environ 24(6):852–860
52. Tawfiq NF, Jaleel J (2015) Radon concentration in soil and radon exhalation rate at Al-Dora refinery and surrounding area in Baghdad. Detection 3(04):37